Environmental Technology & Innovation 29 (2023) 102974

Contents lists available at ScienceDirect

Environmental Technology & Innovation

journal homepage: www.elsevier.com/locate/eti

A novel application of mobile low-cost sensors for atmospheric particulate matter monitoring in open-pit mines

A. Zafra-Pérez [a,*], C. Boente [a,*], A. Sánchez de la Campa [a], J.A. Gómez-Galán [b], J.D. de la Rosa [a]

[a] CIQSO-Center for Research in Sustainable Chemistry, Associate Unit CSIC-University of Huelva "Atmospheric Pollution", Campus El Carmen s/n, 21071 Huelva, Spain

[b] Department of Electronic Engineering, Computers and Automation, University of Huelva, Huelva 21007, Spain

ARTICLE INFO

Article history:
Received 6 October 2022
Received in revised form 14 November 2022
Accepted 25 November 2022
Available online 29 November 2022

Keywords:
PM_{10}
Sensor
Calibration
Air pollution
Mining

ABSTRACT

Open-pit mines are an important source of atmospheric particulate matter (PM) owing to the constant earth-moving and crushing. The well-known association between high PM concentrations and adverse health effects has made the permanent control of fugitive emissions from mines a public health concern. Nevertheless, the large size of these mines renders this task difficult and expensive to perform with regulatory apparatuses; subsequently, the mining industry requires other technologies with a suitable quality/price ratio. In this study, a novel methodology for the space–time monitoring of PM concentrations in open-pit mines using mobile low-cost sensors (LCSs) is proposed. The study was carried out in the renowned mine of Riotinto for three years (2019–2021). It included a detailed calibration of the mobile LCSs that fulfilled the European/US standards. Time tendency diagrams determined the maximum PM concentrations emitted (≈1600 μg PM_{10}/m^3) and also the seasonal variations. The spatial distribution also revealed the main sources of PM within the mine, which were the mining pit, mineral processing plant, spoil heap of fine materials, and main mining tracks. Finally, the integration of these data together with meteorological information allowed the discovery of the routes of escape of fugitive emissions from the mine toward nearby populations: toward W-SW, with concentrations primarily ranging between 50–100 μg PM_{10}/m^3 and 20–50 μg $PM_{2.5}/m^3$. The results of this research are important as mobile LCSs seem to solve the issue of fugitive emissions monitoring in mining ambiances and will aid the exploitations to become more environmentally friendly.

1. Introduction

The World Health Organization has declared that atmospheric particulate matter (PM) is responsible for 4.2 million premature deaths every year (World Health Organization, 2018), thus confirming atmospheric pollution to be a threat to global public health. Epidemiological researchers have found that prolonged exposure to PM can result in multiple negative effects on health, including respiratory ailments such as lung cancer (Clark et al., 2010; Zhou et al., 2015; Falcon-Rodriguez et al., 2016; Raaschou-Nielsen et al., 2016), cardiovascular mortality (Burnett et al., 2018), and more adverse consequences in newborns (Lee et al., 2013; Klepac et al., 2018). Concerns over the negative effects of PM on health have prompted

* Corresponding authors.
E-mail addresses: adrian.zafra@dfaie.uhu.es (A. Zafra-Pérez), carlos.boente@dimme.uhu.es (C. Boente).

https://doi.org/10.1016/j.eti.2022.102974

legislation worldwide (e.g., Europe, Directive 2008/50/EU, China, MEP, 2012 or the USA, U.S. Environmental Protection Agency, 2012), with the establishment of threshold concentrations for fine (<2.5 μm, $PM_{2.5}$) and coarse (<10 μm, PM_{10}) PM, thereby aiming to control the devastating consequences of air pollution (World Health Organization, 2021).

PM concentrations in the air have traditionally been measured and monitored using fixed-site air quality stations equipped with regulatory apparatuses that despite being extremely precise, have frequent prohibitive costs of acquisition, operation, and maintenance (Brauer et al., 2019; Brauer, 2010; Pope et al., 2011). Therefore, these stations were limited to spar locations in large cities or to specific points of interest (Apte and Pant, 2019). However, in certain studies involving microenvironments (e.g., offices, industrial plants, underground mines), a higher degree of scale and resolution is needed because concentrations of PM can vary significantly at very small distances and during short periods (Snyder et al., 2013). Hence, more complex problems require higher spatial resolution for air pollutants. In this context, recent technological advances have led to the proliferation of mobile low-cost sensors (LCSs) for air quality monitoring (Borghi et al., 2017; McKercher et al., 2017). These have emerged as a novel and promising technology that has increasingly been used for monitoring small-scale $PM_{10}/PM_{2.5}$ concentrations and air pollution assessment because they can easily be transported with mobile platforms, such as cars or unmanned aerial vehicles (UAVs) (Van den Bossche et al., 2015; Apte et al., 2017; Pang et al., 2021; Yu et al., 2022).

Nevertheless, a critical issue involving air pollution monitoring through mobile LCSs must be acknowledged, which is the reliability of the data. Laboratory and field tests have revealed that the performance of these LCSs may vary substantially between different models or even between different units within the same model (Singh et al., 2021; Levy Zamora et al., 2019; Hagan et al., 2018; Kelly et al., 2017). Therefore, calibration of the devices is mandatory to ensure correct measurements. This is frequently done by comparing the results of mobile LCSs with the above-mentioned fixed-site stations (Riley et al., 2016; Tessum et al., 2018). It is worth mentioning that calibrations have greatly been improved in recent years, sometimes by complex mathematical algorithms, and it has become possible to obtain very accurate results (Báthory et al., 2022; Zimmerman et al., 2018; Spinelle et al., 2017, 2015). Thus, networks of LCSs have begun to be established and scientifically approved. LCSs have been included in massive air quality monitoring networks, namely large-scale applications, promoted by governments and private corporations, such as the USA's Imperial County Community Air Monitoring Network (English et al., 2017), the Community Air Sensor Network Southeast (CAIRSENSE, Jiao et al., 2016), or the Swiss "Open-Sense" network (Hasenfratz et al., 2015). There are also applications on a mid-scale, referred to specific contexts where mobile LCSs have also been successfully implemented and where there are no other solutions for the permanent monitoring of PM concentrations in 3D space. For instance, Rodríguez and López-Darias (2021) used LCSs to assess the stratification of Saharan dust in Santo Antão island (785 km^2). In another study, Popoola et al. (2018) used mobile LCSs to assess the contribution of air traffic to air pollution at London Heathrow Airport (12.14 km^2).

The novelty of mobile LCS is that they allow to provide information of PM concentrations every second at any location, being very useful as warning systems against dust emissions in places where potentially toxic PM is highly produced and permanent monitoring is required. In line with these mid-scale applications, it was found that mines are indisputable sources of PM, sometimes even containing high concentrations of potentially toxic elements (Patra et al., 2016; Noble et al., 2017; Gautam et al., 2018; Roy et al., 2019). Therefore, PM monitoring is very important to protect the health of workers and individuals residing in surrounding areas in light of possible environmental disasters involving health urgencies (Johnson et al., 2019; Mpanza et al., 2022). Surprisingly, this simple task cannot be adequately performed because of the lack of technologies for the permanent monitoring of PM in mines, which hampers the possibility of controlling fugitive emissions. More specifically, this study aimed to provide researchers and mining companies with a novel methodology to spatially control the distribution of PM based on the data obtained from mobile LCSs regularly transported within the mining facilities by pickup trucks for three years (2019–2021). The present study was carried out in the large and prestigious mine of Riotinto (18.74 km^2). In this place, Boente et al. (2022) reported a considerable amount of PM released by mining operations, and its impact was reflected in populations residing nearby (Sánchez de la Campa et al., 2020). Therefore, this area was optimal for the development of this innovative application of mobile LCSs that has never been tested before.

2. Materials and methods

2.1. Study area

The Riotinto mining district (Huelva, Spain; Fig. 1) is one of the largest polymetallic sulfide open-pit mines in the world (Leistel et al., 1997). It is located in the Iberian Pyrite Belt (sub-Portuguese section), and its predominant ores are pyrite, chalcopyrite, arsenopyrite, sphalerite, and galena. The main metal exploited was copper (Cu), with a mean ore grade of 0.42% (Tornos, 2006). This prominent mineral wealth attracted various international corporations that kept the mine operational between 1873 and 2001, when it closed by profit motives. However, the mine was reactivated in 2015 because of the novel technological advances that allowed the exploitation of ores of low grade, up to 0.20%; currently, approximately 9000 people reside in three towns surrounding the exploited mine (Instituto de Estadística y Cartografía de Andalucía, 2021).

The low-grade ores exploited required hard earth and rock movements. Moreover, the mine was large (approximately 20 km^2 in area). The climate was dry with low precipitation, and the area was mountainous, with strong winds throughout

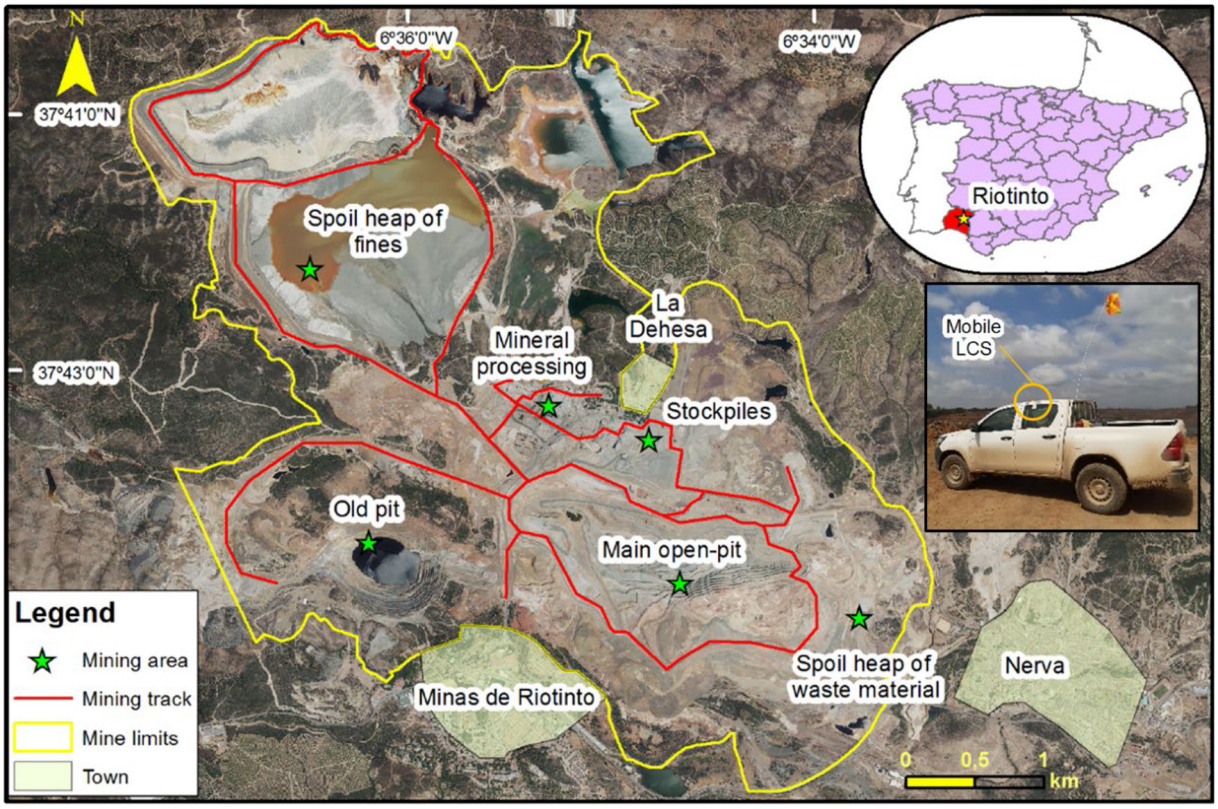

Fig. 1. Location of the Riotinto mine in Huelva, Spain. Vehicles used and position of the mobile Low-cost sensor. Mining tracks for the routes and the different mining areas they crossed.

the year. All these factors encouraged the production of high amounts of PM. Thus, air pollution was considered to be one of the main environmental concerns in the Riotinto mining district (Sánchez de la Campa et al., 2020).

To control air quality, mining companies implemented emission abatement systems for controlling fugitive emissions into the atmosphere. The main technology used was irrigation performed with water neutralized with calcium carbonate from the mining processes. The production of Cu in the Riotinto mine in 2021 was 56,139 tons after treating the plant with 15.8 million tons of mineral, one million more than the year before (ATYM, 2021). Thus, the main sources of PM were open-pit mining operations and mineral processing plants (Boente et al., 2022). The main areas of the mine are shown in Fig. 1.

2.2. Mobile LCSs

Data acquisition was performed using a single low-cost (<300 USD) and consumer-based unit for the entire study (Badura et al., 2019). The unit contains a PMS7003 internal optical particle sensor from Plantower Co. LTD. (Beijing, China) to measure the PM, with dimensions of $13.23 \times 9.83 \times 2.79$ cm and a weight of 142 g. The detectable particle sizes are smaller than 10, 2.5, and 1 μm (namely PM_{10}, $PM_{2.5}$ and PM_1, respectively), and the effective range of detectable particle concentrations is from 0 to 500 $\mu g/m^3$, with a maximum consistency error of ±10% at 100–500 $\mu g/m^3$, a resolution of 1 $\mu g/m^3$, and durability of more than three years. Additionally, the device also has a relative humidity (RH) sensor (HIH-5030-001, Honeywell, Golden Valley, Minnesota) with an accuracy of ±3% RH (max.) at 11%–89% RH and a temperature (T) sensor (MCP9700T-E/TT, Microchip, Arizona, USA) with an accuracy of ±4 °C (max.) at 0–70 °C. All three sensors have a 1 s time resolution and a 2000 mAh 3.7 V rechargeable lithium battery that can power the instrument for 10 h when fully charged. Using Bluetooth®, the device can be paired with a smartphone (Android© OS) running the AirCasting app (aircasting.org). At the end of each mobile session, the data collected from PM, RH, and *T* were sent to a free and open-source platform, Crowdmap, where the data were combined with geographic coordinates collected by GPS (Google Maps©) to generate heat maps that indicated where the PM concentrations were highest and lowest, making the device a mobile LCSs.

2.3. Calibration of mobile LCSs and validation

The mobile LCSs for PM used in this study (Plantower PMS7005) were originally calibrated using a standard aerosol (ISO 12103 – A1, 2016), outdoors in the Arizona Desert (USA). The physical properties of this material and the climatic conditions in the study area were different from those in the Riotinto mine. For this reason, some authors have highlighted the importance of proper calibration prior to its use utilizing regulatory apparatuses and emulating workplace conditions (Giordano et al., 2021).

Prior to the start of the sampling campaign, a comprehensive calibration of the PM sensor Plantower PMS7003 was carried out following the recommendations of previous researchers (Badura et al., 2018), the EPA (U.S. Environmental Protection Agency, 2021a), and EU protocols (EU Working Group, 2010). This was done by means of an outdoor field campaign for 64 days (24 h per day, totalizing 1536 h) using two apparatuses located in an official air quality monitoring station belonging to the Andalusian government. The station is located at 55 km in straight line in the city of Huelva, which presents the same climate conditions, due to availability of equipment, it was not possible to calibrate it in a closest area. Thus, mobile LCSs were measured simultaneously with (1) a beta attenuation 5014i model (Thermo Scientific, Franklin, USA, UNE-EN 16450, 2017), with a resolution of 0.1 $\mu g/m^3$, equipped with a smart heathy system. This is a piece of fixed-site monitoring equipment that offer continuous and real-time measurements of PM_{10} and $PM_{2.5}$ concentrations with a time resolution of 1 s. (2) a regulatory (UNE-EN 12341, 2015) high-volume air sampler (MCV CAVF-PM1025, 30 m^3 h^{-1}, Barcelona, Spain) equipped with PM_{10} and $PM_{2.5}$ Munktell quartz fiber filters that collect PM for 24 h. PM_{10} and $PM_{2.5}$ concentrations were determined in the laboratory following the gravimetric standard procedure (UNE-EN 12341, 2015).

The process of data treatment for calibration was the same as that used by some researchers (Zimmerman, 2022; U.S. Environmental Protection Agency, 2021b; Kang et al., 2017). It consisted of a time resolution transformation: data from mobile LCSs and beta attenuation devices are directly comparable because they have the same time resolution (1 s); however, to make both comparable with the high-volume air sampler (MCV), which has a different time resolution (24 h), all 1 s measures from mobile LCSs and beta attenuation device needed to be averaged for the same 24 h period.

Afterwards, the quality of calibration was carried out via linear regression between (1) the mobile LCSs and beta attenuation device and (2) mobile LCSs and MCV. These two linear regressions were compared to the results obtained by other researchers. Once approved, a calibration factor was extracted from mobile LCSs and MCV regressions. Owing to this calibration factor, it was possible to correct the PM raw data directly measured by the mobile LCSs, thus obtaining similar results to those obtained by the regulatory apparatuses.

Finally, up to five goodness-of-fit statistical indicators were used to validate whether the corrected LCS $PM_{10}/PM_{2.5}$ concentrations are more proxy for reality than the raw LCS concentrations (Table SM1). Researchers have previously applied all these to fine PM air sensors (Gressent et al., 2020; Wu et al., 2020). The indicators are the mean bias (MB), normalized mean bias (NMB), root mean square error (RMSE), normalized mean error (NME), and normalized root mean square error (NRMSE).

Another issue involving mobile LCSs is their behavior after multiple hours of use. PM measurements can worsen over time because of the effect of drift. In this respect, although studies by authors such as Mukherjee et al. (2017) showed that Plantower PMS7003 has a long precision even in the long term, others noticed that it can undergo damages that may affect the quality of the measurements in the long term under certain outdoor conditions (Bulot et al., 2019). In this study, the drift was quantified for PM_{10} using the results from beta attenuation 5014i. Thus, following the EPA protocols (U.S. Environmental Protection Agency, 2021b), data were selected from the first and the last five days of the total 64 days that the calibration lasted for. Differences were established through linear regression for the first and last five days (Unal-Palmira, 2019; U.S. Environmental Protection Agency, 2021b).

2.4. Sampling campaign

The sampling campaign with the mobile LCSs was conducted for three years (January 2019–December 2021). In 2019, 69 samplings were carried out, corresponding to one per week and two during summer, which is a dryer season than winter. In 2020, two samples were collected every week for a total of 110 samplings. In 2021, the frequency increased to three per week for a total of 155 samples. Thus, 334 samples were collected over the three years. The condition of no sampling during rainfall events was imposed in order to avoid the influence of rain that would distort results and interpretations.

Each sampling corresponded to a route across the mine with the mobile LCSs located on the side of a pickup truck (Fig. 1), ensuring that the particles suspended by driving do not reach the sensor. The route in the mining vehicle was always covered at a low speed (<30 km/h), which was the maximum speed allowed by the mining company. In this context, Gressent et al. (2020) stated that up to 50 km/h, the motion of the vehicle does not affect the measurement of the mobile LCSs. Higher speeds cause errors in the measurements, and speeds of more than 80 km/h contest the validity of the data acquired. After each sampling, the mobile LCS is stored in a metal box at 20 °C to prevent deterioration of the equipment.

The route consisted of a long-distance tour across a mine with a duration of 1 h. It crossed the main mining tracks, mineral processing plants, berms, and spoil heaps of coarse and fine materials. When covering the route, pickup trucks frequently encountered operators performing typical mining activities, such as mining machine traffic, drilling, and loading of ore and waste material. It is worth mentioning that the track may change slightly because the mine is constantly evolving and mining tracks are frequently getting modified. However, these areas, which were identified as the main sources of atmospheric PM in a previous study (Boente et al., 2022), were always crossed.

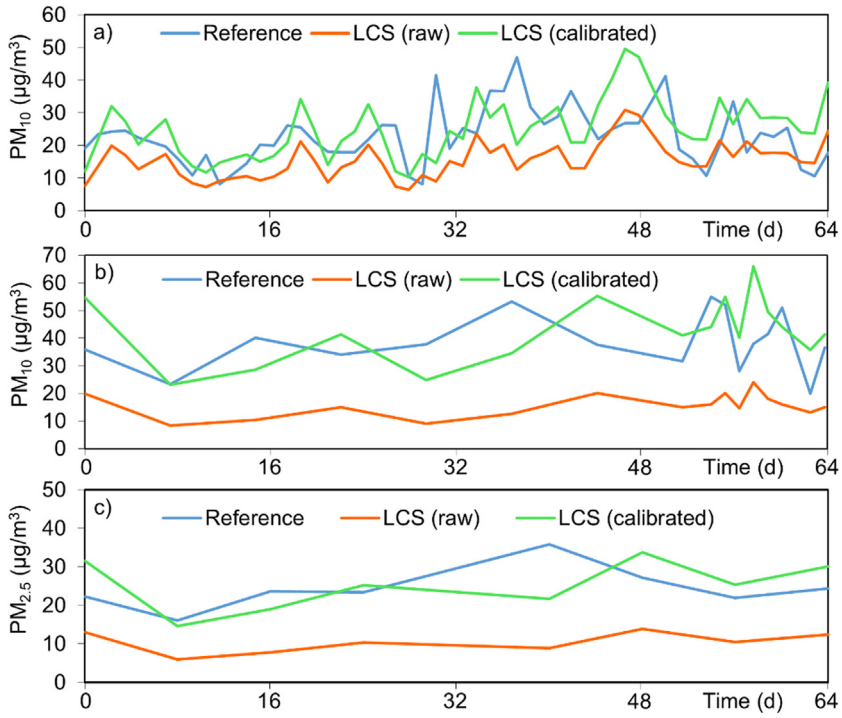

Fig. 2. (a) Intercomparison between mobile LCSs and beta attenuation 5014i (Reference). Average PM_{10} concentrations for 24 h. (b) Intercomparison between mobile LCSs and MCV CAVF-PM102 (Reference). Average PM_{10} concentrations for 24 h. (c) Intercomparison between mobile LCSs and MCV CAVF-PM102 (Reference). Average $PM_{2.5}$ concentrations for 24 h. . (For interpretation of the references to color in this figure legend, the reader is referred to the web version of this article.)

2.5. Data treatment

Hourly data for the meteorological parameters were obtained from the MeteoBlue© platform. MeteoBlue© is a software that assembles meteorological data from different models (NEMSGLOBAL, ERA5, NEMS12 *y* NEMS4, ICON, among others, Müller, 2021), from series ranging from 1984 to today through the premium package *History+*. The meteorological station selected was Nerva (37.696°N 6.550°W, 336 m.a.s.l.), the one closest among those available to the Riotinto mine (3 km). The spatial resolution is 30 km (between 1984 and 2007) and 4 km (from 2008 to now). Although the platform can provide multiple meteorological parameters (e.g., T, precipitation, radiation), in this study, there were exclusively extracted wind speed and wind direction. All data related to wind speed and direction were introduced in the statistical package OpenAir (Carslaw, 2021; Carslaw and Ropkins, 2012), constructed with the integrated development environment of RStudio (RStudio Team, 2020). OpenAir offers a rapid and versatile series of R scripts that provide graphical outputs of time series for meteorological data, which can substantially support the interpretation of the study results. For the present research, the following OpenAir commands were used to obtain different graphical outputs: calculate nonparametric smooth trends (Function smoothTrend), diurnal, day of the week, monthly variation (timeVariation), pollution rose variation (pollutionRose), and flexible scatter plots (scatterPlot). Additionally, a principal component analysis (PCA) was performed using SPSS v.22 to study the relationship between these variables. As proposed for geochemical data (Reimann and de Caritat, 2005), the varimax/orthogonal rotation was used to extract factors using the Kaiser/Gutmann criterion.

3. Results and discussion

3.1. Evaluation of mobile LCS monitoring in the mining environment

After calibration was performed as described in Section 2.3, first, the results for the intercomparison between the mobile LCSs under examination and the apparatuses already installed (the beta attenuation 5014i device and the regulatory MCV CAVF-PM1025 High-Volume Air Sampler) are shown (Fig. 2). At first glance, PM data corresponding to calibrated data (green) overlap more with the reference (blue) lines than with the raw data (orange). Indeed, after collating raw data, it was observed that, by default, the mobile LCSs underestimate the risk-providing concentrations that are most of the time below those provided by official apparatuses. With the new calibration, this has been corrected.

Table 1
Results of linear regression between mobile LCSs ($PM_{2.5}$ Plantower PMS7003) and MCV CAVF-PM102 for $PM_{2.5}$ filters.

Source	Sensor	Slope	Intersection	R^2
Badura et al. (2018)		3.57	−11.82	0.91
(AQ-SPEC, 2016)	Plantower	1.35	−7.21	0.84
Unal-Palmira (2019)	PMS7003	0.56	−8.48	0.44
Frederick et al. (2020)		Not provided	Not provided	0.47
Mukherjee et al. (2017)	$PM_{2.5}$	0.36	4.91	0.62
Own		0.71	−4.95	0.83

Table 2
Average 24 h concentration of PM_{10} for the raw and calibrated data in the reference equipment and the mobile LCSs during the calibration. Deviations for goodness-of-fit statistical indicators for raw and calibrated data.

PM_{10} ($\mu g/m^3$)	Beta Atte. 24 h		MCV 24 h	
Reference ($\mu g/m^3$)	22.9		40.2	
	Raw	Calibrated	Raw	Calibrated
Mobile LCSs ($\mu g/m^3$)	15.6	25.1	16.2	44.4
Statistical indicators	Deviations			
MB ($\mu g/m^3$)	−7.29	2.21	−24.0	4.25
NMB (%)	−31.9	9.66	−59.8	10.6
RMSE ($\mu g/m^3$)	11.3	10.5	27.8	18.4
NME (%)	36.8	36.5	59.7	38.2
NRMSE (%)	49.5	45.9	69.1	45.8

In this context, the results obtained from the calibration of $PM_{2.5}$ were excellent when compared to the calibrations performed in other studies via linear regression (Table 1). For instance, the $R^2 = 0.83$ for $PM_{2.5}$ MCV CAVF-PM102 filters is the third best adjustment among other calibrations for the same sensor. These results are acceptable as it is a comparison between equipment that measures everything that accumulates in the $PM_{10}/PM_{2.5}$ filters every second for over 24 h. These differences are frequently attributed to climatic conditions. Malings et al. (2020) detected that RH, T, and high concentrations of PM may negatively affect measurements by LCSs. Based on this, Magi et al. (2020) confirmed that high RH may change the refraction indices of atmospheric PM and lead to their hygroscopic growth, inducing errors in the measurements.

To evaluate how the calibrated data fit the real measure, goodness-of-fit statistical indicators were applied apart from R^2. For $PM_{2.5}$, some international organizations involving air pollution, such as the EU (EU Working Group, 2010), the United Kingdom (Breathe London, 2019), and the United States (U.S. Environmental Protection Agency, 2021a) have delimited threshold errors for goodness-of-fit statistical indicators. These are summarized in Table SM2, where it can be observed that the calibrated LCS values fulfill the objectives established in the USEPA recommendations for slope, the intersection of the calibration line, R^2, RMSE, and NRMSE statistical indicators (U.S. Environmental Protection Agency, 2021b). All the calibrated data were highly improved in comparison to the raw data. Therefore, this calibration was optimal for $PM_{2.5}$.

Regarding the calibration of PM_{10} measurements, Table 2 shows a comparison between the different statistical indicators calculated using raw and calibrated data. The average concentration of PM_{10} for the calibrated data in the mobile LCSs was a better proxy to those of the reference equipment than the raw data. Moreover, the deviations obtained for the statistical indicators were lower for the calibrated data. According to Gressent et al. (2020), the following requirements must be fulfilled with these statistical indicators: $MB \leq NMB \leq RMSE \leq NME \leq NRMSE$, to ensure a correct measure of the concentration of PM_{10} by the sensor. This condition is fulfilled in this case: $4.25 \leq 10.6 \leq 18.4 \leq 38.2 \leq 45.8$. Thus, it is concluded that the calibration resulted in an improvement, and the calibrated data obtained will be similar to those obtained by the reference equipment for PM_{10}.

Once the measures of the mobile LCSs are precise, it is necessary to describe the drift that it undergoes after running for hours. The drift assessment performed in this study for 64 days (1536 h) resulted in a reduction of 5.6% in PM_{10} concentrations during the last five days of the calibration campaign, concerning the first five. In the study of drift performed by EPA (U.S. Environmental Protection Agency, 2021b), which lasted for 64 days (1536 h), researchers found evidence of drift when comparing the first five days to the last five. In this case, it resulted in a decrease of 6.5% in the concentration of PM. These results are similar to those presented here. However, the sampling campaign comprised 334 routes with an approximate duration of 1 h (total 334 h). Thus, assuming that the drift follows a linear decrease in time, as suggested by (Unal-Palmira, 2019), the real PM concentrations during the last samplings of 2021 would be 1.2% lower than those in the first samplings in 2019, an error that can be considered acceptable. Thus, additional correction of the final data was performed in this respect.

Table 3
Annual mean levels (January 2019–December 2021) for PM_{10} and $PM_{2.5}$ obtained via mobile LCSs in the Riotinto mine.

Year	Number of routes	Duration	PM_{10} ($\mu g/m^3$)					$PM_{2.5}$ ($\mu g/m^3$)				
			Mean	Std	RSD	Min	Max	Mean	Std	RSD	Min	Max
2019	69	1 h 13 min	55	23	42	3	1042	25	11	44	2	270
2020	110	1 h 5 min	84	35	42	5	1578	35	11	33	4	304
2021	155	1 h 1 min	84	31	37	5	1588	32	11	35	4	280
2019–21	334	1 h 6 min	78	33	42	3	1588	32	12	37	3	304

3.2. Trends of PM_{10} and $PM_{2.5}$ concentrations

The previous calibrations allowed corrections of the raw data obtained by the mobile LCSs. Hereafter, every result corresponded to the accurate data found in the study area. The annual average PM_{10} and $PM_{2.5}$ concentrations for each of the years of study are summarized in Table 3. For PM_{10}, the year 2019 registered mean concentrations of 55 $\mu gPM_{10}/m^3$, a number that increased by 55% during the next year, 2020 (rising up to 84 $\mu gPM_{10}/m^3$). This fact was consistent with the increase in the production in the Riotinto mine: from 10.5 million tons in 2019 to 14.8 million tons in 2020 (ATYM, 2021). In 2021, even with a more intense sampling campaign, the mean concentration was equal to the previous year (84 $\mu gPM_{10}/m^3$) in spite of the mine getting treated with more materials (15.8 million tons, ATYM, 2021), indicating a better control of the PM. The maximum concentrations registered also increased from 1042 $\mu gPM_{10}/m^3$ in 2019 to 1588 $\mu gPM_{10}/m^3$ in 2021. For $PM_{2.5}$, the trends were practically similar. The mean concentration in 2019 (25 $\mu gPM_{2.5}/m^3$) was lower than that in 2020 (35 $\mu gPM_{2.5}/m^3$) and 2021 (32 $\mu gPM_{2.5}/m^3$). However, the proportion of $PM_{2.5}/PM_{10}$ ranges between 39%–45%. In the event of extreme or maximum concentration, this proportion diminishes to 17%–26%. This should present low values because the finest particles are more hazardous to health.

With respect to the statistical reliability of the data, a standard deviation that was always regular and below the mean was observed. The relative standard deviations were approximately between 33 and 44% for both PM_{10} and $PM_{2.5}$, which reveals consistency in the measures with the mobile LCSs. The extreme values appearing in the maxima can be therefore considered to be punctual and limited to specific locations, which can be easily identified owing to the GPS features of the mobile LCSs.

Additionally, Fig. 3 reveals the increase in PM concentrations over time using tendency diagrams. Box whisker plots showing the variation by months and weekdays can be found in Supplementary Materials (Figures SM1, SM2 and SM3). Obtaining all these figures would be unconceivable in the absence of a LCS. The one represented in Fig. 3a clarifies the distribution of PM_{10} and $PM_{2.5}$ throughout the study period. PM_{10} concentrations varied widely depending on the month. The maximum means for each year were found in July: 80 $\mu gPM_{10}/m^3$ in 2019, 100 $\mu gPM_{10}/m^3$ in 2020, and 95 $\mu gPM_{10}/m^3$ in 2021. In this context, the diagram reveals that the concentrations of PM can be duplicated during summer months concerning the concentrations during winter months: approximately 40 $\mu gPM_{10}/m^3$ in all the years. Another aspect that Fig. 3a reveals is that the tendency of PM_{10} concentrations increased significantly from 2019 to 2020 and remained stable during 2021, a fact that was mentioned before and was coincident with the intensification of production of PM in mines. Moreover, the COVID-19 pandemic's containment, which occurred in Spain during March–June 2020, did not have an effect on the production of PM in this mine.

With respect to the concentrations of $PM_{2.5}$, the tendency was similar to that of PM_{10} but on a smaller scale. Fluctuations between summer and winter months still existed, but were less evident, and the data were generally more consistent. Major peaks were also found in July. However, the increase in $PM_{2.5}$ observed in 2020 and 2021 was not as significant as that observed in PM_{10}.

Taking advantage of the degree of detail that these LCSs can reach, it was possible to identify those months and days where the production of PM is intensified (Fig. 3b). Thus, the months with the highest production of PM are months of summer (June, July, and August) and those with the lowest are months of winter. Considering the days of the week, it was found that the Riotinto mine produced a similar degree of PM by the years, around 70–100 $\mu gPM_{10}/m^3$ in 2020–2021 and 45–65 $\mu gPM_{10}/m^3$ in 2019.

Taking all these into consideration, it can be concluded that 2020 and 2021 were similar in terms of dust production, and the mine will need to apply measures for dust abatement if levels of 2019 are desired, which is especially worrying during the summer months. Considering the strong bond observed between PM and climatic seasons, it is worthwhile to study certain climate variables associated with air pollution to deeply understand the reasons for these variations in PM concentrations. Thus, the T and RH from the mobile LCSs and wind speed data from MeteoBlue© were compared with the mean PM_{10} concentrations for each of the 334 routes. For this part of the study, no data of $PM_{2.5}$ is used since the coarsest material (PM_{10}) is considerably more present and $PM_{2.5}$ follows its same tendency, also in accordance with previous results as well as other research studies (Boente et al., 2022; Sánchez de la Campa et al., 2020).

The comparative analysis started with factor analysis (PCA and varimax rotation) to assess the linkages between variables (Table 4). PM_{10} appears in both Factor 1 and Factor 2, showing a positive correlation with T and wind speed and a negative correlation with RH. This implies that high T, high wind speeds, and RH are favorable conditions for obtaining high concentrations of PM_{10} in mines. However, for these results, it should be taken into consideration that although

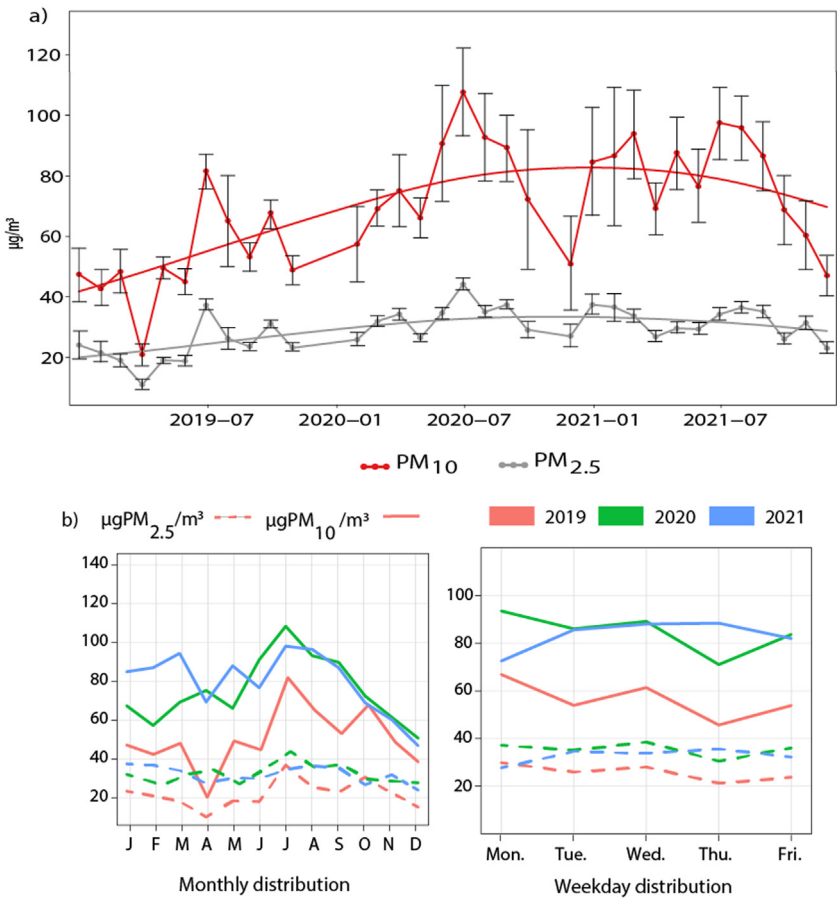

Fig. 3. (a) Tendency diagram for PM_{10} and $PM_{2.5}$ for the whole period of 2019–2021. Each point represents the mean of the corresponding month and standard deviation is represented by vertical lines. (b) Monthly and weekday distribution of PM_{10} and $PM_{2.5}$ for each year.

Table 4
Factor loadings and percentage of variance explained by the varimax-rotated factors extracted by principal components and communalities.

Variable	F1	F2	Communality
Mean T	0.912	−0.101	0.842
Mean RH	−0.814	0.075	0.669
Mean PM_{10}	0.539	0.455	0.498
Mean wind speed	−0.149	0.902	0.836
% Variance explained (Accumulated)	45.264	71.119	–

the percentage of variance explained is relatively high (71%), the communality and the factor loadings for PM_{10} are low (0.498).

A visual representation of this finding is shown in Fig. 4. Each point in the figure represents a single route. The colors of the climate variable and the position over the *y*-axis represents the concentration of PM_{10}. The highest concentrations were reached during the months with the highest *T* (Fig. 4a, red points), whereas the majority of routes covered on cold days (blue points) had concentrations below 100 $\mu g/m^3$, with some exceptions in 2021. A better definition is appreciated when considering the RH (Fig. 4b). Routes covered under a high value of RH (>80%) tended to have PM_{10} concentrations of approximately 50 $\mu g/m^3$, whereas the highest concentrations were reached under a low RH value. Discussing the effect of RH on particles, Badura et al. (2018) stated that the impact of high relative humidity level was observed for LCS above 80% RH. Apart, Jayaratne et al. (2018) confirmed that it is in conditions close to the 100% RH, when the formation of fog or mist may occur and the water droplets may be detected as particle by the mobile LCS. In the present study, values tend to be below 80% (Fig. 4b), so the inference of RH is minimal. Finally, the wind speed diagram (Fig. 4c) showed that high concentrations of PM_{10} were reached when the wind speed was high. This is because strong winds cause PM lifting, thus provoking a dispersion effect of particles.

Fig. 4. Mean PM_{10} dispersion diagram during 2019–2021 for (a) temperature, (b) relative humidity, and (c) wind speed. Each point represents a route. . (For interpretation of the references to color in this figure legend, the reader is referred to the web version of this article.)

3.3. Spatial distribution of PM_{10} and $PM_{2.5}$

The mobile LCS performs measurements every second. This allows the concentration of PM to be mapped to assess where higher concentrations of PM_{10} and $PM_{2.5}$ are located and support the search for solutions to reduce emissions. Fig. 5 shows the mean concentrations of PM_{10} and $PM_{2.5}$, respectively, for each year and all periods. Pollution roses represent the main direction of the wind and the dispersion of PM considering their concentration.

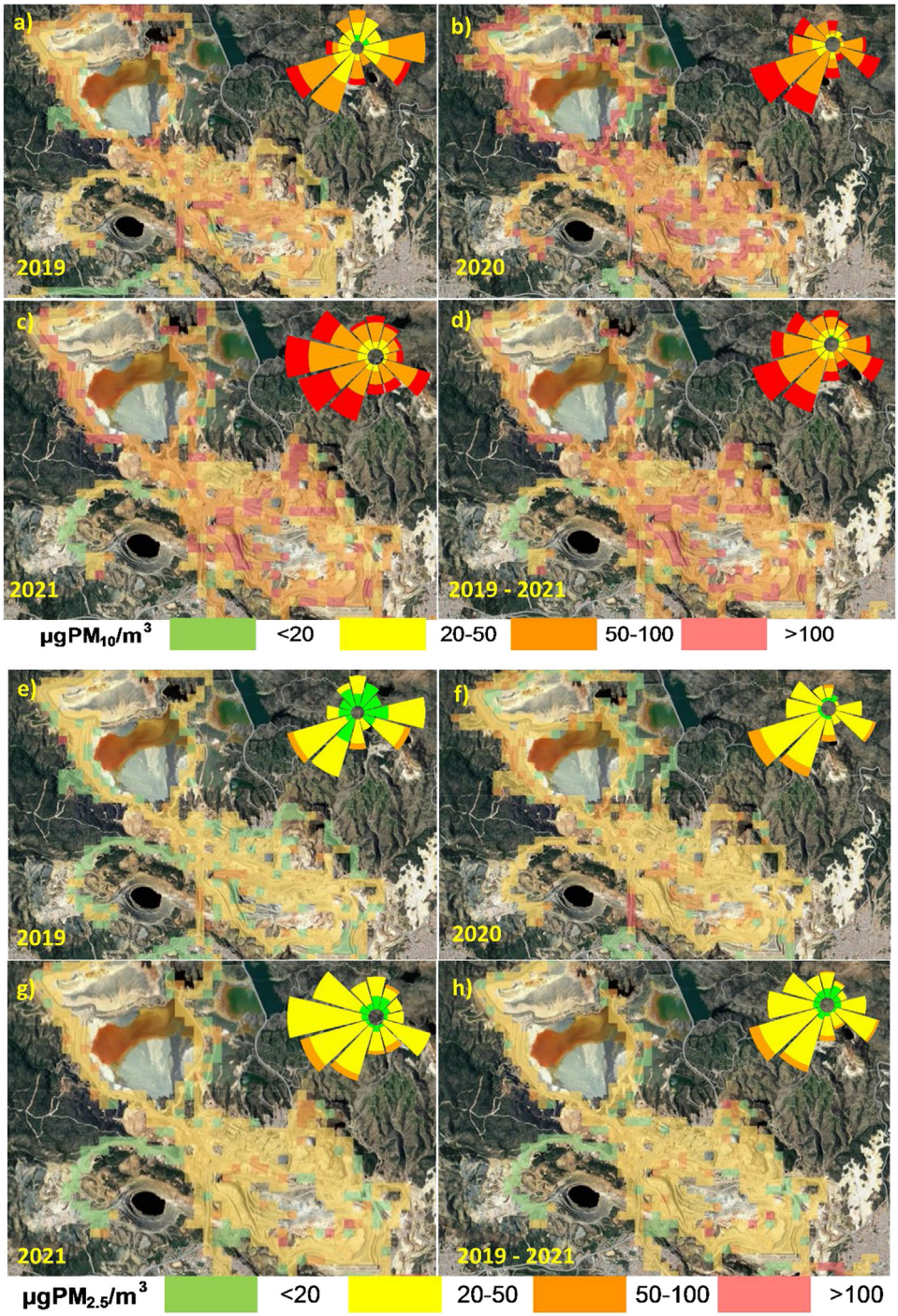

Fig. 5. (a) to (d): Spatial distribution for PM_{10} in different periods of study; (e) to (h): Spatial distribution for $PM_{2.5}$ in different periods of the study. Wind roses for the periods of study are also included.

Based on the mean distribution of PM_{10} (Fig. 5(a) to (d)), it was observed that the concentrations generally surpassed 50 $\mu g/m^3$ in practically the entire mine area, with some areas surpassing 100 $\mu g/m^3$. Among these are the spoil heap of fine materials (a), mining pit (b), mineral processing plant (c), and main mining tracks (d). Analyzing every year, 2020 was the year with the highest surface area, when concentration surpassed 100 $\mu gPM_{10}/m^3$. 2021 was similar, and both years presented higher PM_{10} concentrations than 2019 in practically the entire mine area. The maps were very

similar for the entire period. With respect to $PM_{2.5}$ (Fig. 5(e) to (h)), as it has been previously observed, the pattern is the same as that of PM_{10} but with lower concentrations. There were practically no changes during the three years, although the concentrations were moderate (20–50 $\mu gPM_{2.5}/m^3$) and practically disappeared within the limits of the mine ($<$20 $\mu gPM_{10}/m^3$), which implied a low dispersion of the finest particles outside the mine. In this context, the significantly higher concentrations of PM_{10} in comparison with $PM_{2.5}$ reveal that coarse particles are predominant in the study area. Although further conclusions about PM distribution cannot be obtained without the use of a cascade impactor, all these values are far from those that can be obtained by haulage in underground metallic mining, which can surpass 350 $\mu gPM_{10}/m^3$ (Paluchamy and Mishra, 2021).

Concerning this dispersion, winds were predominant in the W-SW direction during the entire study period. Thus, the majority of PM_{10} and $PM_{2.5}$ will travel toward these ranges of directions in the abovementioned high concentrations. In this way, the town of Minas de Riotinto is located, with a population of approximately 4000 inhabitants.

Thus, the predominant concentrations within the mine of Riotinto are high for PM_{10} (approximately 50–100 $\mu g/m^3$) and moderate for $PM_{2.5}$ (20–50 $\mu g/m^3$). To the best of the authors' knowledge, mobile LCSs have not been previously applied in mines. Subsequently, it is not possible to offer results from other similar studies to discuss and give readers a global idea of the magnitude of the concentrations in this source of pollution. However, studies implementing mobile LCSs in other fields have shown interesting results. For instance, forest fires can emit a daily mean exceeding 100 $\mu gPM_{2.5}/m^3$ (Sayahi et al., 2019). Another field study performed with a network of mobile LCSs stated that spatiotemporal variations in the large city of Xi'an (China) may range between 2 and 413 $\mu gPM_{2.5}/m^3$ (Gao et al., 2015). In another city in China (Cangzhou), a network of mobile LCSs coupled with taxis allowed the mapping of pollution in the entire city and obtained values surpassing 250 $\mu gPM_{2.5}/m^3$ (Wu et al., 2020).

The mine in Riotinto, as shown in the previous maps (Fig. 5), is far from reaching the majority of the levels mentioned above. The harm the mine can cause is not attributable to excessive PM concentrations but to the permanent activity and the punctual extreme peaks of PM that specific mining operations can produce, the point where mobile LCSs could play a key role with their constant surveillance and their competitive quality/price ratio. To reduce the PM concentrations in those identified concerning locations, measures like punctual irrigation through $CaCO_3$-neutralized water from mining processes, or creating a film of impervious material to retain dust via bitumen from polymers or Portland cement can be used to reduce the impact of PM pollution in surface (Darling, 2011). However, these concentrations were studied within the surface of the mine. In future research, these types of mobile LCSs can be transported using UAVs, and the scattering at different altitudes can be addressed to evaluate the final concentrations that reach the neighboring populations.

4. Conclusion

The use of mobile LCSs has increased in recent times because it allows the permanent monitoring of air quality parameters in known coordinates at a very low cost. Their utility has been previously proven in multiple applications but never in open-pit mining, which is a prominent source of PM. In this study, atmospheric pollution caused by PM_{10} and $PM_{2.5}$ was addressed by means of mobile LCS after a comprehensive calibration that included intercomparison with MCV high-volume air sampler and beta attenuation devices. With the calibrated mobile LCS, we stated that it is possible to detect the location and time of peak concentrations, as well as to perform tendency diagrams to study the evolution of PM during different seasons, months, or days; thus, locating points of maximum dust production with high precision. In these areas, measures for dust abatement, such as water irrigation, may be introduced.

Moreover, mobile LCSs frequently measure other parameters, such as T or RH. This information, statistically treated together with other climate data, such as wind speed or wind direction, allows to discern the climate conditions that encourage the appearance of the highest concentrations, which is undoubtedly useful for preventing days when maximum concentrations may compromise the health of humans. In the case of Riotinto, favorable conditions were high T, low RH, and high wind speed. Finally, the GPS system integrated in the mobile LCSs allowed the mapping of the spatial distribution of PM_{10}/ $PM_{2.5}$ and to identify those areas of the mine that are the highest emitters of PM. In Riotinto, these were the mining pit, mineral processing plant, spoil heap of fine material, and main mining tracks. Moreover, it was possible to assess the escape of fugitive emissions by combining data from mobile LCSs and meteorological information to assess the impact of the mine on nearby populations. In this study, the scattering of PM was predominantly in the W-SW direction, with concentrations primarily ranging between 50–100 $\mu gPM_{10}/m^3$ and 20–50 $\mu gPM_{2.5}/m^3$.

This vast amount of information was gathered with a degree of detail that would be unaffordable with the regulatory methods of air quality monitoring. In this context, with the proper calibration mobile LCSs can show results in the same level to other more precise air quality monitoring devices, such as a high-volume air sampler or a beta attenuation equipment. However, the function of mobile LCS is not substitute but to complement their results by providing measures every second with GPS functionality, which allows the fast identification of concerning areas in such a way this novel application might be very useful for mining companies.

All things considered, mobile LCSs have strong potential for permanent dust control in open-pit mining. They can operate as an early warning system to act against extreme events or can be used to study areas where the concentrations of PM are high to implement measures for dust abatement, such as irrigation or ventilation, and to protect the health of workers and people residing in the surroundings of the mine.

CRediT authorship contribution statement

A. Zafra-Pérez: Writing – original draft, Investigation, Data curation, Formal analysis, Software, Visualization. **C. Boente:** Writing – original draft, Investigation, Methodology, Validation, Supervision. **A. Sánchez de la Campa:** Writing – review & editing, Supervision. **J.A. Gómez-Galán:** Writing – review & editing, Resources, Supervision. **J.D. de la Rosa:** Writing – review & editing, Resources, Conceptualization, Methodology, Supervision, Funding acquisition, Project administration.

Declaration of competing interest

The authors declare that they have no known competing financial interests or personal relationships that could have appeared to influence the work reported in this paper.

Data availability

The authors do not have permission to share data.

Acknowledgments

The authors are grateful to Atalaya Mining Company for giving the permission to carry out this research on their facilities and for their active support. Carlos Boente obtained a post-doctoral contract within the program PAIDI 2020 (Ref 707 DOC 01097) and the PY18-2332 Project, co-financed by the Junta de Andalucía (Andalusian Government), Spain and the EU. Funding for open access charge: Universidad de Huelva/CBUA, Spain.

Appendix A. Supplementary data

Supplementary material related to this article can be found online at https://doi.org/10.1016/j.eti.2022.102974.

References

Air Quality Sensor Performance Evaluation Center, 2016. Available at: http://www.aqmd.gov/aq-spec.

Apte, J.S., Messier, K.P., Gani, S., Brauer, M., Kirchstetter, T.W., Lunden, M.M., Marshall, J.D., Portier, C.J., Vermeulen, R.C.H., Hamburg, S.P., 2017. High-resolution air pollution mapping with google street view cars: Exploiting big data. Environ. Sci. Technol. 51, 6999–7008. http://dx.doi.org/10.1021/acs.est.7b00891.

Apte, J.S., Pant, P., 2019. Toward cleaner air for a billion Indians. Proc. Natl. Acad. Sci. 116, 10614–10616. http://dx.doi.org/10.1073/pnas.1905458116.

ATYM, 2021. Consolidated and Company Financial Assessments. p. 4.

Badura, M., Batog, P., Drzeniecka-Osiadacz, A., Modzel, P., 2018. Evaluation of low-cost sensors for ambient PM 2.5 monitoring. J. Sensors 2018, 1–16. http://dx.doi.org/10.1155/2018/5096540.

Badura, M., Batog, P., Drzeniecka-Osiadacz, A., Modzel, P., 2019. Regression methods in the calibration of low-cost sensors for ambient particulate matter measurements. SN Appl. Sci. 1, 622. http://dx.doi.org/10.1007/s42452-019-0630-1.

Báthory, C., Dobó, Z., Garami, A., Palotás, Á., Tóth, P., 2022. Low-cost monitoring of atmospheric PM—development and testing. J. Environ. Manag. 304, 114158. http://dx.doi.org/10.1016/j.jenvman.2021.114158.

Boente, C., Millán-Martínez, M., Sánchez de la Campa, A.M., Sánchez-Rodas, D., de la Rosa, J.D., 2022. Physicochemical assessment of atmospheric particulate matter emissions during open-pit mining operations in a massive sulphide ore exploitation. Atmos. Pollut. Res. 13, 101391. http://dx.doi.org/10.1016/j.apr.2022.101391.

Borghi, F., Spinazzè, A., Rovelli, S., Campagnolo, D., Cattaneo, A., Cavallo, D., 2017. Miniaturized monitors for assessment of exposure to air pollutants: A review. Int. J. Environ. Res. Public Health 14, 909. http://dx.doi.org/10.3390/ijerph14080909.

Brauer, M., 2010. How much, how long, what, and where: Air pollution exposure assessment for epidemiologic studies of respiratory disease. Proc. Am. Thorac. Soc 7, 111–115. http://dx.doi.org/10.1513/pats.200908-093RM.

Brauer, M., Guttikunda, S.K., KA, N., Dey, S., Tripathi, S.N., Weagle, C., Martin, R.V., 2019. Examination of monitoring approaches for ambient air pollution: A case study for India. Atmos. Environ. 216, 116940. http://dx.doi.org/10.1016/j.atmosenv.2019.116940.

Bulot, F.M.J., Johnston, S.J., Basford, P.J., Easton, N.H.C., Apetroaie-Cristea, M., Foster, G.L., Morris, A.K.R., Cox, S.J., Loxham, M., 2019. Long-term field comparison of multiple low-cost particulate matter sensors in an outdoor urban environment. Sci. Rep. 9, 7497. http://dx.doi.org/10.1038/s41598-019-43716-3.

Burnett, R., Chen, H., Szyszkowicz, M., Fann, N., Hubbell, B., Pope, C.A., Apte, J.S., Brauer, M., Cohen, A., Weichenthal, S., Coggins, J., Di, Q., Brunekreef, B., Frostad, J., Lim, S.S., Kan, H., Walker, K.D., Thurston, G.D., Hayes, R.B., Lim, C.C., Turner, M.C., Jerrett, M., Krewski, D., Gapstur, S.M., Diver, W.R., Ostro, B., Goldberg, D., Crouse, D.L., Martin, R.V., Peters, P., Pinault, L., Tjepkema, M., van Donkelaar, A., Villeneuve, P.J., Miller, A.B., Yin, P., Zhou, M., Wang, L., Janssen, N.A.H., Marra, M., Atkinson, R.W., Tsang, H., Quoc Thach, T., Cannon, J.B., Allen, R.T., Hart, J.E., Laden, F., Cesaroni, G., Forastiere, F., Weinmayr, G., Jaensch, A., Nagel, G., Concin, H., Spadaro, J.V., 2018. Global estimates of mortality associated with long-term exposure to outdoor fine particulate matter. Proc. Natl. Acad. Sci. 115, 9592–9597. http://dx.doi.org/10.1073/pnas.1803222115.

Carslaw, D., 2021. OpenAir: Tools for the analysis of air pollution data.

Carslaw, D.C., Ropkins, K., 2012. Openair — An R package for air quality data analysis. Environ. Model. Softw. 27–28, 52–61. http://dx.doi.org/10.1016/j.envsoft.2011.09.008.

Clark, N.A., Demers, P.A., Karr, C.J., Koehoorn, M., Lencar, C., Tamburic, L., Brauer, M., 2010. Effect of early life exposure to air pollution on development of childhood asthma. Environ. Health Perspect. 118, 284–290. http://dx.doi.org/10.1289/ehp.0900916.

Darling, P., 2011. SME Mining Engineering Handbook. Society for Mining, Metallurgy, and Exploration, Englewood, Colo.

English, P.B., Olmedo, L., Bejarano, E., Lugo, H., Murillo, E., Seto, E., Wong, M., King, G., Wilkie, A., Meltzer, D., Carvlin, G., Jerrett, M., Northcross, A., 2017. The imperial county community air monitoring network: A model for community-based environmental monitoring for public health action. Environ. Health Perspect. 125, 074501. http://dx.doi.org/10.1289/EHP1772.

EU Working Group, 2010. Guide to the demonstration of equivalence of ambient air monitoring methods. https://ec.europa.eu/environment/air/quality/legislation/pdf/equivalence.pdf (accessed 8.10.22).

Falcon-Rodriguez, C.I., Osornio-Vargas, A.R., Sada-Ovalle, I., Segura-Medina, P., 2016. Aeroparticles, composition, and lung diseases. Front. Immunol. 7, http://dx.doi.org/10.3389/fimmu.2016.00003.

Frederick, S., Johnson, K., Johnson, C., Yaga, R., Clements, A., 2020. Performance evaluations of PM2.5 sensors in Research Triangle Park, NC: PurpleAir PA-II-SD, Aeroqual AQY, Applied Particle Technology Maxima, Vaisala AQT420, sens-it RAMP, and clarity node-S. https://cfpub.epa.gov/si/si_public_record_report.cfm?Lab=CEMM&dirEntryId=348487 (accessed 8.10.22).

Gao, M., Cao, J., Seto, E., 2015. A distributed network of low-cost continuous reading sensors to measure spatiotemporal variations of PM2.5 in Xi'an, China. Environ. Pollut. 199, 56–65. http://dx.doi.org/10.1016/j.envpol.2015.01.013.

Gautam, S., Patra, A.K., Sahu, S.P., Hitch, M., 2018. Particulate matter pollution in opencast coal mining areas: a threat to human health and environment. Int. J. Min. Reclam. Environ. 32, 75–92. http://dx.doi.org/10.1080/17480930.2016.1218110.

Giordano, M.R., Malings, C., Pandis, S.N., Presto, A.A., McNeill, V.F., Westervelt, D.M., Beekmann, M., Subramanian, R., 2021. From low-cost sensors to high-quality data: A summary of challenges and best practices for effectively calibrating low-cost particulate matter mass sensors. J. Aerosol Sci. 158, 105833. http://dx.doi.org/10.1016/j.jaerosci.2021.105833.

Gressent, A., Malherbe, L., Colette, A., Rollin, H., Scimia, R., 2020. Data fusion for air quality mapping using low-cost sensor observations: Feasibility and added-value. Environ. Int. 143, 105965. http://dx.doi.org/10.1016/j.envint.2020.105965.

Hagan, D.H., Isaacman-VanWertz, G., Franklin, J.P., Wallace, L.M.M., Kocar, B.D., Heald, C.L., Kroll, J.H., 2018. Calibration and assessment of electrochemical air quality sensors by co-location with regulatory-grade instruments. Atmos. Meas. Tech. 11, 315–328. http://dx.doi.org/10.5194/amt-11-315-2018.

Hasenfratz, D., Saukh, O., Walser, C., Hueglin, C., Fierz, M., Arn, T., Beutel, J., Thiele, L., 2015. Deriving high-resolution urban air pollution maps using mobile sensor nodes. Pervasive Mob. Comput. 16, 268–285. http://dx.doi.org/10.1016/j.pmcj.2014.11.008.

Instituto de Estadística y Cartografía de Andalucía, 2021. Multiterritorial information system of Andalusia. https://www.juntadeandalucia.es/institutodeestadisticaycartografia/sima/provincia.htm?prov=21 (accessed 8.10.22).

ISO 12103 – A1, 2016. Fine test dust. Filtration standards & specifications.

Jayaratne, R., Liu, X., Thai, P., Dunbabin, M., Morawska, L., 2018. The influence of humidity on the performance of a low-cost air particle mass sensor and the effect of atmospheric fog. Atmos. Meas. Tech. 11, 4883–4890. http://dx.doi.org/10.5194/amt-11-4883-2018.

Jiao, W., Hagler, G., Williams, R., Sharpe, R., Brown, R., Garver, D., Judge, R., Caudill, M., Rickard, J., Davis, M., Weinstock, L., Zimmer-Dauphinee, S., Buckley, K., 2016. Community Air Sensor Network (CAIRSENSE) project: evaluation of low-cost sensor performance in a suburban environment in the southeastern United States. Atmos. Meas. Tech. 9, 5281–5292. http://dx.doi.org/10.5194/amt-9-5281-2016.

Johnson, A.L., Dipnall, J.F., Dennekamp, M., Williamson, G.J., Gao, C.X., Carroll, M.T.C., Dimitriadis, C., Ikin, J.F., Johnston, F.H., McFarlane, A.C., Sim, M.R., Stub, D.A., Abramson, M.J., Guo, Y., 2019. Fine particulate matter exposure and medication dispensing during and after a coal mine fire: A time series analysis from the Hazelwood Health Study. Environ. Pollut. 246, 1027–1035. http://dx.doi.org/10.1016/j.envpol.2018.12.085.

Kang, G., Kim, J.-J., Kim, D.-J., Choi, W., Park, S.-J., 2017. Development of a computational fluid dynamics model with tree drag parameterizations: Application to pedestrian wind comfort in an urban area. Build. Environ. 124, 209–218. http://dx.doi.org/10.1016/j.buildenv.2017.08.008.

Kelly, K.E., Whitaker, J., Petty, A., Widmer, C., Dybwad, A., Sleeth, D., Martin, R., Butterfield, A., 2017. Ambient and laboratory evaluation of a low-cost particulate matter sensor. Environ. Pollut. 221, 491–500. http://dx.doi.org/10.1016/j.envpol.2016.12.039.

Klepac, P., Locatelli, I., Korošec, S., Künzli, N., Kukec, A., 2018. Ambient air pollution and pregnancy outcomes: A comprehensive review and identification of environmental public health challenges. Environ. Res. 167, 144–159. http://dx.doi.org/10.1016/j.envres.2018.07.008.

Lee, P.-C., Roberts, J.M., Catov, J.M., Talbott, E.O., Ritz, B., 2013. First trimester exposure to ambient air pollution, pregnancy complications and adverse birth outcomes in Allegheny County, PA. Matern. Child Health J. 17, 545–555. http://dx.doi.org/10.1007/s10995-012-1028-5.

Leistel, J.M., Marcoux, E., Thiéblemont, D., Quesada, C., Sánchez, A., Almodóvar, G.R., Pascual, E., Sáez, R., 1997. The volcanic-hosted massive sulphide deposits of the Iberian Pyrite Belt. Miner. Depos. 33, 2–30. http://dx.doi.org/10.1007/s001260050130.

Levy Zamora, M., Xiong, F., Gentner, D., Kerkez, B., Kohrman-Glaser, J., Koehler, K., 2019. Field and laboratory evaluations of the low-cost plantower particulate matter sensor. Environ. Sci. Technol. 53, 838–849. http://dx.doi.org/10.1021/acs.est.8b05174.

Magi, B.I., Cupini, C., Francis, J., Green, M., Hauser, C., 2020. Evaluation of PM2.5 measured in an urban setting using a low-cost optical particle counter and a federal equivalent method beta attenuation monitor. Aerosol Sci. Technol. 54, 147–159. http://dx.doi.org/10.1080/02786826.2019.1619915.

Malings, C., Tanzer, R., Hauryliuk, A., Saha, P.K., Robinson, A.L., Presto, A.A., Subramanian, R., 2020. Fine particle mass monitoring with low-cost sensors: Corrections and long-term performance evaluation. Aerosol Sci. Technol. 54, 160–174. http://dx.doi.org/10.1080/02786826.2019.1623863.

McKercher, G.R., Salmond, J.A., Vanos, J.K., 2017. Characteristics and applications of small, portable gaseous air pollution monitors. Environ. Pollut. 223, 102–110. http://dx.doi.org/10.1016/j.envpol.2016.12.045.

MEP, 2012. Ministry of environmental protection of the People's Republic of China. Ambient air quality standards. https://www.transportpolicy.net/standard/china-air-quality-standards/ (accessed 8.10.22).

Mpanza, M., Adam, E., Moolla, R., 2022. The potential health costs of PM10 impacts on a gold mine village, during company liquidation: An analysis of 2013–2017. Minerals 12 (169), http://dx.doi.org/10.3390/min12020169.

Mukherjee, A., Stanton, L., Graham, A., Roberts, P., 2017. Assessing the utility of low-cost particulate matter sensors over a 12-week period in the Cuyama Valley of California. Sensors 17 (1805), http://dx.doi.org/10.3390/s17081805.

Müller, M., 2021. Meteoblue: weather close to you. https://www.meteoblue.com/ (accessed 8.10.22).

Noble, T.L., Parbhakar-Fox, A., Berry, R.F., Lottermoser, B., 2017. Mineral dust emissions at metalliferous mine sites. In: Environmental Indicators in Metal Mining. Springer International Publishing, Cham, pp. 281–306. http://dx.doi.org/10.1007/978-3-319-42731-7_16.

Paluchamy, B., Mishra, D.P., 2021. Airborne dust generation and dispersion profiles due to loaded LPDT haulage in decline of a highly mechanized underground lead–zinc ore mine. Environ. Technol. Innov. 24, 101908. http://dx.doi.org/10.1016/j.eti.2021.101908.

Pang, X., Chen, L., Shi, K., Wu, F., Chen, J., Fang, S., Wang, J., Xu, M., 2021. A lightweight low-cost and multipollutant sensor package for aerial observations of air pollutants in atmospheric boundary layer. Sci. Total Environ. 764, 142828. http://dx.doi.org/10.1016/j.scitotenv.2020.142828.

Patra, A.K., Gautam, S., Kumar, P., 2016. Emissions and human health impact of particulate matter from surface mining operation—A review. Environ. Technol. Innov. 5, 233–249. http://dx.doi.org/10.1016/j.eti.2016.04.002.

Pope, C.A., Brook, R.D., Burnett, R.T., Dockery, D.W., 2011. How is cardiovascular disease mortality risk affected by duration and intensity of fine particulate matter exposure? An integration of the epidemiologic evidence. Air Qual. Atmos. Health 4, 5–14. http://dx.doi.org/10.1007/s11869-010-0082-7.

Popoola, O.A.M., Carruthers, D., Lad, C., Bright, V.B., Mead, M.I., Stettler, M.E.J., Saffell, J.R., Jones, R.L., 2018. Use of networks of low cost air quality sensors to quantify air quality in urban settings. Atmos. Environ. 194, 58–70. http://dx.doi.org/10.1016/j.atmosenv.2018.09.030.

Raaschou-Nielsen, O., Beelen, R., Wang, M., Hoek, G., Andersen, Z.J., Hoffmann, B., Stafoggia, M., Samoli, E., Weinmayr, G., Dimakopoulou, K., Nieuwenhuijsen, M., Xun, W.W., Fischer, P., Eriksen, K.T., Sørensen, M., Tjønneland, A., Ricceri, F., de Hoogh, K., Key, T., Eeftens, M., Peeters, P.H., Bueno-de Mesquita, H.B., Meliefste, K., Oftedal, B., Schwarze, P.E., Nafstad, P., Galassi, C., Migliore, E., Ranzi, A., Cesaroni, G., Badaloni, C., Forastiere, F., Penell, J., De Faire, U., Korek, M., Pedersen, N., Östenson, C.-G., Pershagen, G., Fratiglioni, L., Concin, H., Nagel, G., Jaensch, A., Ineichen, A., Naccarati, A., Katsoulis, M., Trichpoulou, A., Keuken, M., Jedynska, A., Kooter, I.M., Kukkonen, J., Brunekreef, B., Sokhi, R.S., Katsouyanni, K., Vineis, P., 2016. Particulate matter air pollution components and risk for lung cancer. Environ. Int. 87, 66–73. http://dx.doi.org/10.1016/J.Envint.2015.11.007.

Reimann, C., de Caritat, P., 2005. Distinguishing between natural and anthropogenic sources for elements in the environment: regional geochemical surveys versus enrichment factors. Sci. Total Environ. 337, 91–107. http://dx.doi.org/10.1016/j.scitotenv.2004.06.011.

Riley, E.A., Schaal, L., Sasakura, M., Crampton, R., Gould, T.R., Hartin, K., Sheppard, L., Larson, T., Simpson, C.D., Yost, M.G., 2016. Correlations between short-term mobile monitoring and long-term passive sampler measurements of traffic-related air pollution. Atmos. Environ. 132, 229–239. http://dx.doi.org/10.1016/j.atmosenv.2016.03.001.

Rodríguez, S., López-Darias, J., 2021. Dust and tropical PMx aerosols in Cape Verde: Sources, vertical distributions and stratified transport from North Africa. Atmos. Res. 263, 105793. http://dx.doi.org/10.1016/j.atmosres.2021.105793.

Roy, D., Singh, G., Seo, Y.-C., 2019. Carcinogenic and non-carcinogenic risks from PM10-and PM2.5-Bound metals in a critically polluted coal mining area. Atmos. Pollut. Res. 10, 1964–1975. http://dx.doi.org/10.1016/j.apr.2019.09.002.

RStudio Team, 2020. R: A Language and Environment for Statistical Computing. R Foundation for Statistical Computing, Vienna, Austria.

Sánchez de la Campa, A.M., Sánchez-Rodas, D., Márquez, G., Romero, E., de la Rosa, J.D., 2020. 2009–2017 Trends of PM10 in the legendary Riotinto mining district of SW Spain. Atmos. Res. 238, 104878. http://dx.doi.org/10.1016/j.atmosres.2020.104878.

Sayahi, T., Butterfield, A., Kelly, K.E., 2019. Long-term field evaluation of the Plantower PMS low-cost particulate matter sensors. Environ. Pollut. 245, 932–940. http://dx.doi.org/10.1016/j.envpol.2018.11.065.

Singh, D., Dahiya, M., Kumar, R., Nanda, C., 2021. Sensors and systems for air quality assessment monitoring and management: A review. J. Environ. Manag. 289, 112510. http://dx.doi.org/10.1016/j.jenvman.2021.112510.

Snyder, E.G., Watkins, T.H., Solomon, P.A., Thoma, E.D., Williams, R.W., Hagler, G.S.W., Shelow, D., Hindin, D.A., Kilaru, V.J., Preuss, P.W., 2013. The changing paradigm of air pollution monitoring. Environ. Sci. Technol. 47, 11369–11377. http://dx.doi.org/10.1021/es4022602.

Spinelle, L., Gerboles, M., Villani, M.G., Aleixandre, M., Bonavitacola, F., 2015. Field calibration of a cluster of low-cost available sensors for air quality monitoring. Part A: Ozone and nitrogen dioxide. Sensors Actuators B 215, 249–257. http://dx.doi.org/10.1016/j.snb.2015.03.031.

Spinelle, L., Gerboles, M., Villani, M.G., Aleixandre, M., Bonavitacola, F., 2017. Field calibration of a cluster of low-cost commercially available sensors for air quality monitoring, Part B: NO, CO and CO2. Sensors Actuators B 238, 706–715. http://dx.doi.org/10.1016/j.snb.2016.07.036.

Tessum, M.W., Larson, T., Gould, T.R., Simpson, C.D., Yost, M.G., Vedal, S., 2018. Mobile and fixed-site measurements to identify spatial distributions of traffic-related pollution sources in Los Angeles. Environ. Sci. Technol. 52, 2844–2853. http://dx.doi.org/10.1021/acs.est.7b04889.

Tornos, F., 2006. Environment of formation and styles of volcanogenic massive sulfides: The Iberian Pyrite Belt. Ore Geol. Rev. 28, 259–307. http://dx.doi.org/10.1016/j.oregeorev.2004.12.005.

Unal-Palmira, 2019. Evaluación Meteorológica, Operacional y Aplicación de Analizadores de Bajo Costo a la Medición de Inmisión y Exposición a Material Particulado PM2.5 en un Sector Residencial y Comercial de sur de Santiago de Cali, Colombia (BSc Thesis). National University of Colombia.

UNE-EN 12341, 2015. Ambient air - Standard gravimetric measurement method for the determination of the PM10 or PM2, 5 mass concentration of suspended particulate matter.

UNE-EN 16450, 2017. Ambient air - Automated measuring systems for the measurement of the concentration of particulate matter (PM10; PM2, 5).

U.S. Environmental Protection Agency, 2012. National ambient air quality standards (NAAQS) for particulate matter (PM).

U.S. Environmental Protection Agency, 2021a. Air monitoring methods - Criteria pollutants.

U.S. Environmental Protection Agency, 2021b. Performance testing protocols, metrics, and target values for fine particulate matter air sensors: Use in ambient, outdoor, fixed site, non-regulatory supplemental and informational monitoring applications.

Van den Bossche, J., Peters, J., Verwaeren, J., Botteldooren, D., Theunis, J., De Baets, B., 2015. Mobile monitoring for mapping spatial variation in urban air quality: Development and validation of a methodology based on an extensive dataset. Atmos. Environ. 105, 148–161. http://dx.doi.org/10.1016/j.atmosenv.2015.01.017.

World Health Organization, 2018. People worldwide breathe polluted air, but more countries are taking action. https://www.who.int/news/item/02-05-2018-9-out-of-10-people-worldwide-breathe-polluted-air-but-more-countries-are-taking-action (accessed 8.10.22).

World Health Organization, 2021. WHO Global Air Quality Guidelines: Particulate Matter (PM2.5 and PM10), Ozone, Nitrogen Dioxide, Sulfur Dioxide and Carbon Monoxide. World Health Organization, https://apps.who.int/iris/handle/10665/345329 (accessed 11.1.22).

Wu, Y., Wang, Y., Wang, L., Song, G., Gao, J., Yu, L., 2020. Application of a taxi-based mobile atmospheric monitoring system in Cangzhou, China. Transp. Res. D 86, 102449. http://dx.doi.org/10.1016/j.trd.2020.102449.

Yu, Y.T., Xiang, S., Li, R., Zhang, S., Zhang, K.M., Si, S., Wu, X., Wu, Y., 2022. Characterizing spatial variations of city-wide elevated PM10 and PM2.5 concentrations using taxi-based mobile monitoring. Sci. Total Environ. 829, 154478. http://dx.doi.org/10.1016/j.scitotenv.2022.154478.

Zhou, M., He, G., Liu, Y., Yin, P., Li, Y., Kan, H., Fan, Maorong, Xue, A., Fan, Maoyong, 2015. The associations between ambient air pollution and adult respiratory mortality in 32 major Chinese cities, 2006–2010. Environ. Res. 137, 278–286. http://dx.doi.org/10.1016/j.envres.2014.12.016.

Zimmerman, N., 2022. Tutorial: Guidelines for implementing low-cost sensor networks for aerosol monitoring. J. Aerosol Sci. 159, 105872. http://dx.doi.org/10.1016/j.jaerosci.2021.105872.

Zimmerman, N., Presto, A.A., Kumar, S.P.N., Gu, J., Hauryliuk, A., Robinson, E.S., Robinson, A.L., 2018. A machine learning calibration model using random forests to improve sensor performance for lower-cost air quality monitoring. Atmos. Meas. Tech. 11, 291–313. http://dx.doi.org/10.5194/amt-11-291-2018.